REPORT DOCUMENTATION PAGE

Form Approved
OMB NO. 0704-0188

1. AGENCY USE ONLY (Leave Blank)	2. REPORT DATE	3. REPORT TYPE AND DATES COVERED
	6/02	Final Technical Report 5/99-3/02 01/5/99 - 31/3/02

4. TITLE AND SUBTITLE
Semiconductor Laser for the 2-5 μm and 7-9 μm Region/Quantum Cascade Lasers

5. FUNDING NUMBERS
DAAD19-99-1-0217

6. AUTHOR(S)
M. Razeghi, S. Slivken, Z. Huang, and A. Evans

7. PERFORMING ORGANIZATION NAME(S) AND ADDRESS(ES)
Northwestern University
Center for Quantum Devices
2225 N. Campus Drive, MLSB Room 4051
Evanston, IL 60208-3129

8. PERFORMING ORGANIZATION REPORT NUMBER

9. SPONSORING / MONITORING AGENCY NAME(S) AND ADDRESS(ES)
U. S. Army Research Office
P.O. Box 12211
Research Triangle Park, NC 27709-2211

10. SPONSORING / MONITORING AGENCY REPORT NUMBER
40016-PH
-1

11. SUPPLEMENTARY NOTES
The views, opinions and/or findings contained in this report are those of the author(s) and should not be construed as an official Department of the Army position, policy or decision, unless so designated by other documentation.

12 a. DISTRIBUTION / AVAILABILITY STATEMENT
Approved for public release; distribution unlimited.

12 b. DISTRIBUTION CODE

13. ABSTRACT (Maximum 200 words)

The quantum cascade laser is one of the strong candidates for a portable mid-infrared light source for a variety of DoD applications. We have seen dramatic improvements in high temperature performance at long wavelengths, including threshold current densities as low as 1.4 kA/cm^2 and peak power outputs greater than 7 W for a single 20 mm aperture. Along with the significant design improvements, we have also demonstrated laser operation at 9 and 11 mm up to 425 K. Single mode operation has been accomplished with the use of surface distributed feedback gratings. An important parallel development to these performance improvements is the integration of discrete lasers into a compact, durable laser pointer system. A compact, battery-driven power supply has been designed and tested, as well as a simple, laboratory optical system for pointer evaluation.

14. SUBJECT TERMS	15. NUMBER OF PAGES
	12
	16. PRICE CODE

17. SECURITY CLASSIFICATION OR REPORT	18. SECURITY CLASSIFICATION ON THIS PAGE	19. SECURITY CLASSIFICATION OF ABSTRACT	20. LIMITATION OF ABSTRACT
UNCLASSIFIED	**UNCLASSIFIED**	**UNCLASSIFIED**	**UL**

NSN 7540-01-280-5500

Standard Form 298 (Rev.2-89)
Prescribed by ANSI Std. 239-18
298-102

Introduction

The mid-infrared (2-12 μm) wavelength region is attractive for many DoD laser applications including: LIDAR, infrared countermeasures, covert target acquisition, remote chemical sensing, and secure point-to-point communication. In order for a laser to be viable for these applications, it should be wavelength versatile. Tunability, or a wide emission range, allows multispectral operation and excellent adaptability to new applications. Small size and a rugged package are also beneficial. Vehicle-mounted lasers, which can demonstrate good performance, cannot access all terrain and are very conspicuous. A smaller, handheld package (<2 kg), would be much more suited to an unpredictable environment. Lastly, reliability is an issue. Room temperature operation and a rugged package both extend lifetime (less mechanical parts) and reduce maintenance requirements (optics realignment).

The quantum cascade laser (QCL) offers potentially all of these characteristics using a mature III-V semiconductor material system such as InP. Laser emission has already been demonstrated in pulsed mode at room temperature for wavelengths ranging from 3-11 μm. Our primary goals are to demonstrate the ultimate potential of this device in terms of high temperature operation, efficiency, and output power, and demonstrate a prototype handheld laser pointer system that can operate at room temperature with low beam divergence (<10 mrad). This interim report details the progress we have made over the past 15 months as well as some of the impending technology we are developing to overcome certain obstacles.

Background and Previous Results

The heart of a QCL is the design of the emitting layers, which is made up of active and injector regions. The active region emits light through intersubband transitions inside conduction band quantum wells. The structure can be varied from a single quantum well to a complex chirped superlattice. In all cases, the wavelength of emitted light is primarily determined by the thickness of the semiconductor layers rather than their bandgap. The design of the active region is complex, and must be optimized for high current density throughput and maximum gain as a function of temperature.

The injector region is responsible both for electron transport through the emitting layers and as an energy filter, which is used to recycle electrons from one active region to the next while minimizing leakage. Both functions are accomplished by confining electrons into a narrow superlattice miniband which only transports electrons of the correct energy. Higher energy electrons are confined due to the superlattice minigap as shown in Figure 1a.

The active and injector region pair can be combined in a serial cascade fashion, which allows electrons to emit multiple photons in their trip through the emitting layers. This is shown schematically in Figure 1b. This design can increase the device efficiency and output power tremendously.

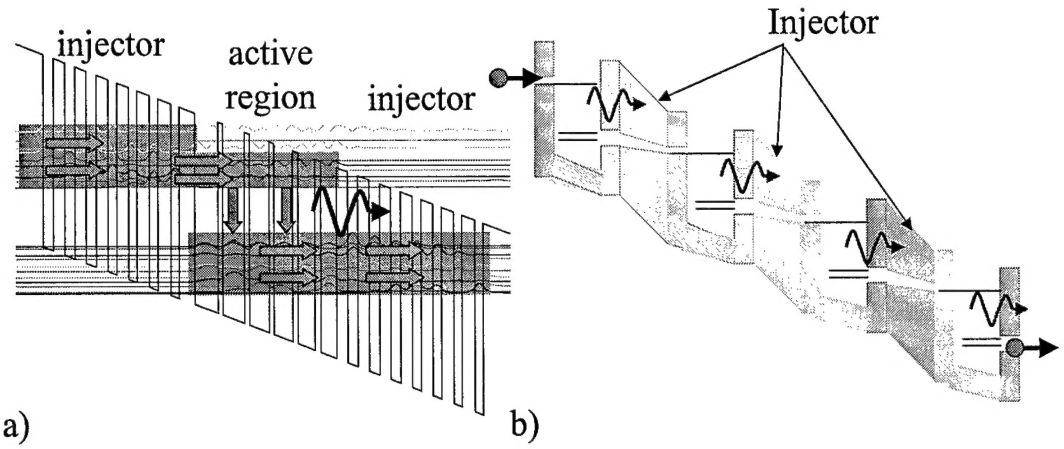

Figure 1 a) Superlattice quantum cascade laser conduction band schematic. b) Cascade operation of serially stacked active/injector stages.

The first quantum cascade laser was produced at the Center for Quantum Devices in a short time after a request by DARPA. Even the initial lasers demonstrated both 5.1 and 8.5 μm laser emission, with the longer wavelength devices operating up to room temperature. Since then, we have made remarkable improvements in the material quality and fabrication technology. As of Jan 2000, we had a variety of results, including the lowest room temperature threshold current density of only 3.4 kA/cm^2 and continuous wave operation up to 140 K. At this point, there was still plenty of room for improvement in design, threshold current density, and output power as will be discussed later in the next section.

Experimental Results

Laser design

As with any device, improving the device design can lead to better performance. In order to maintain a population inversion while minimizing space-charge effects inside the emitting layers, extrinsic carriers need to be supplied. It is well understood, however, that excess doping can lead to increased free-carrier absorption (which scales roughly as λ^2). The proper doping must be established based on the required population inversion, density of states, and steady-state carrier distribution. The last item is difficult to calculate and is highly dependent on the specific active/injector region design.

Our first goal was to find the optimum doping profile and waveguide design for a given emitter structure. A superlattice active region was chosen for this study in order to benefit from a high peak power output and excellent high temperature characteristics. The wavelength was chosen arbitrarily to be 9 μm. The optimization process for this laser should be very similar to any other wavelength, but is a good challenge due to higher losses at longer wavelengths.

The 300 K results are shown in Figure 2 for samples of identical structure, but with different sheet carrier densities. The threshold current density follows a generally linear trend (Figure 2a), with the lowest doping producing the lowest threshold current density of 1.8 kA/cm^2, which is the lowest reported to date for λ>5 μm. The primary reasons for the increase are most likely due to decreased electron leakage (or injection efficiency) and a small increase in waveguide loss. The slope efficiency, however betrays a more complicated behavior, which peaks close to a

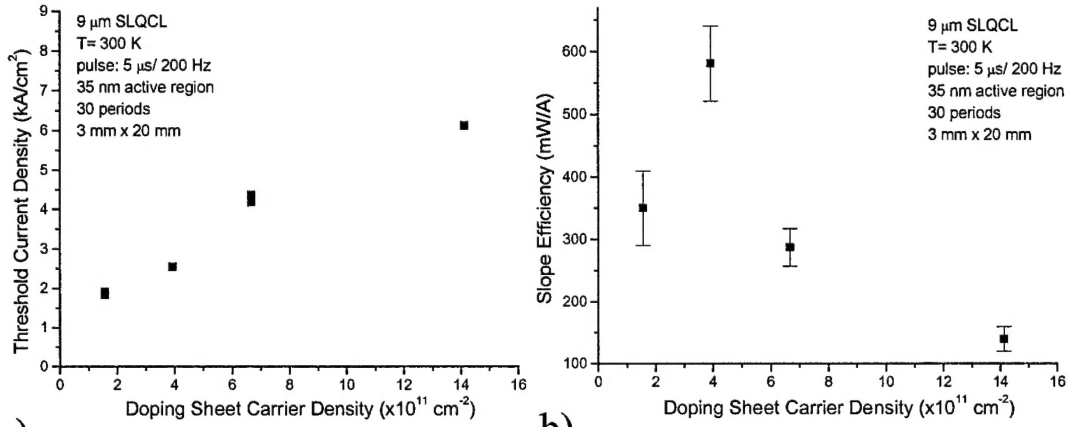

Figure 2 Identical λ=9 μm QCLs engineered with different doping sheet carrier densities. a) Room temperature threshold current density. b) Room temperature slope efficiency.

sheet carrier density of 4x10^{11} cm^{-2}. At lower doping, it is believed the optimum injection condition (injector aligned with the active region) only exists within a narrow voltage/current range near threshold. As the doping increases, this range increases, leading to a higher maximum current density and a higher initial slope efficiency. However, the increased leakage and loss at higher doping quickly overcomes this improvement, leading to the gradual decrease of slope efficiency as shown experimentally in Figure 2b. With this data, specific laser performance can be engineered based on the application. For higher duty cycles at low temperatures, the lowest doping is preferred. For the highest peak power output, a doping level of 4-6 x 10^{11} cm^{-2} produces the best results.

Optimization of the waveguide is also very important to device operation. The general waveguide design principles were studied, and developed into a generic waveguide as shown in Figure 3. This design shows low free-carrier absorption and, with the addition of the highly doped cap layer, helps reduce any loss at the metal-semiconductor interface due to surface plasmon effects.

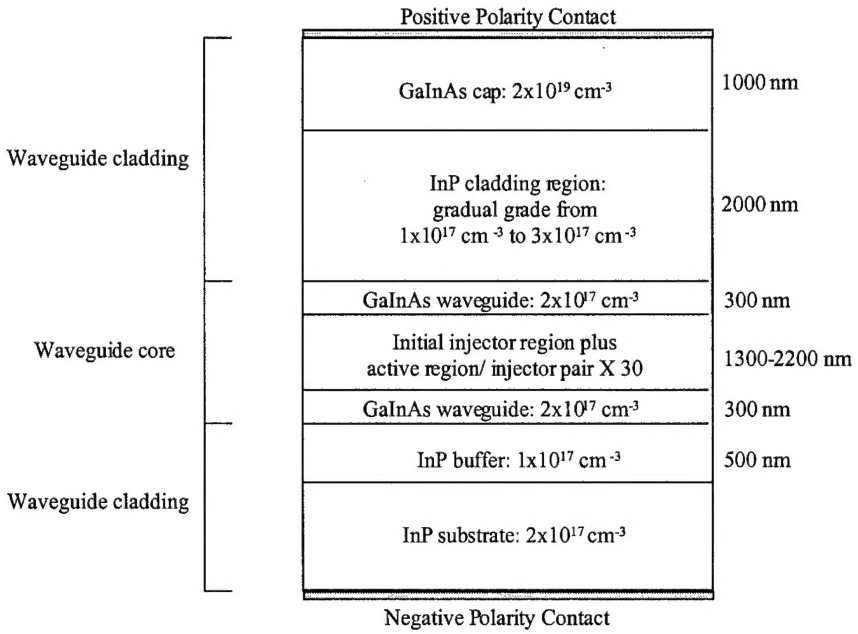

Figure 3 Generic waveguide structure used for 5-12 μm quantum cascade lasers.

Taking into account both phonon- and plasmon-based contributions to the refractive index profile of the waveguide, a complex mode-solver was developed in-house to solve for the both the optical mode and the waveguide losses. The solver uses the transfer matrix method and the argument principle method to find the complex waveguide propagation constants. A single-mode solution for the above generic waveguide design is shown in Figure 4.

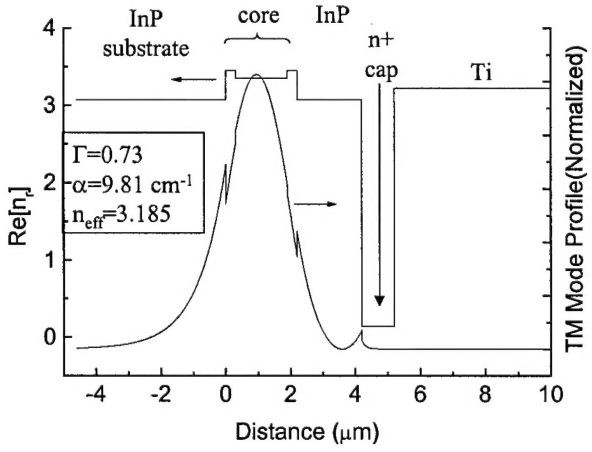

Figure 4 Refractive index and fundamental TM mode profiles for a typical λ= 9 μm QCL waveguide. The effective refractive index is 3.185 with a confinement factor of 73%.

Theoretically, the optical confinement factor and slope efficiency should both scale with the number of emission stages in the waveguide core. We grew a series of the same 9 μm QCL structures studied above with different core thicknesses to increase the peak power output per stripe and study whether or not the growth and

processing are scalable to thicker structures. The peak power increased as predicted up to 75 periods as shown in Figure 5, with no noticeable saturation effects. Using 75 periods, a typical 3 mm laser can generate 7 W peak power per 2 facets at room temperature.

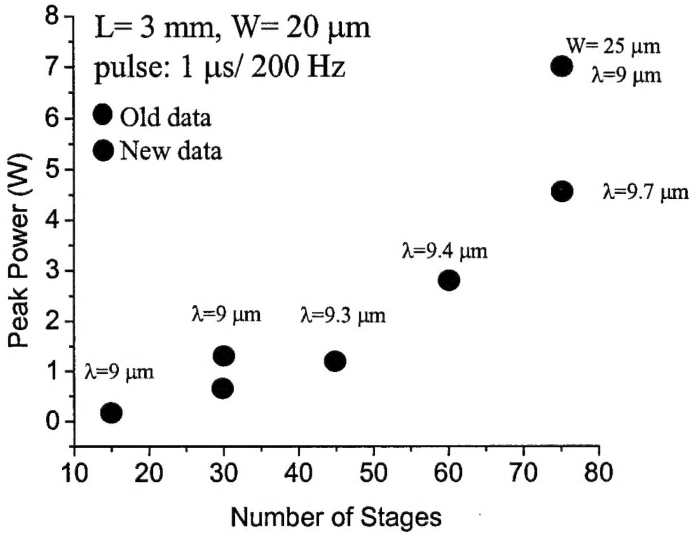

Figure 5 Peak power as a function of the number of stages for a series of 9-10 μm SLQCLs.

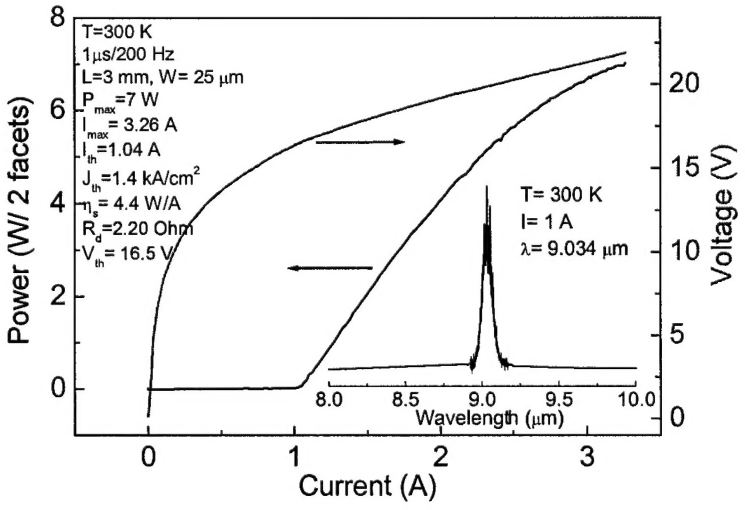

Figure 6 P-I-V behavior of a 75-stage SLQCL. Peak power output is 7 W per 2 facets with a threshold current density of 1.4 kA/cm^2. The inset shows the laser emission spectrum at 9μm near threshold.

The low threshold and high output powers demonstrated by these lasers also scale to longer wavelengths and higher temperatures. At 11 μm, we have demonstrated a

50 period device with 1 W of peak output power at room temperature. Both the 9 and 11 μm lasers have shown laser operation up to 425 K, with power output 2.4 W at 425 K for λ= 9 μm.

Our QCL devices were also tested for average power delivery at room temperature as a function of duty cycle (Figure 7). As predicted, the thermal resistance (R_{th}) of the 75-stage laser is higher than that of the 30-stage laser. This is especially apparent when R_{th} is scaled to area. As a consequence of this and a higher operating voltage, the thermal rollover occurs earlier. However, the maximum average power is still highest for the 75-stage laser, with over 300 mW per 2 facets observed at 300 K. This is currently the highest average power reported for a QCL at room temperature. Clearly, even higher average power can be obtained by reducing the thermal resistance.

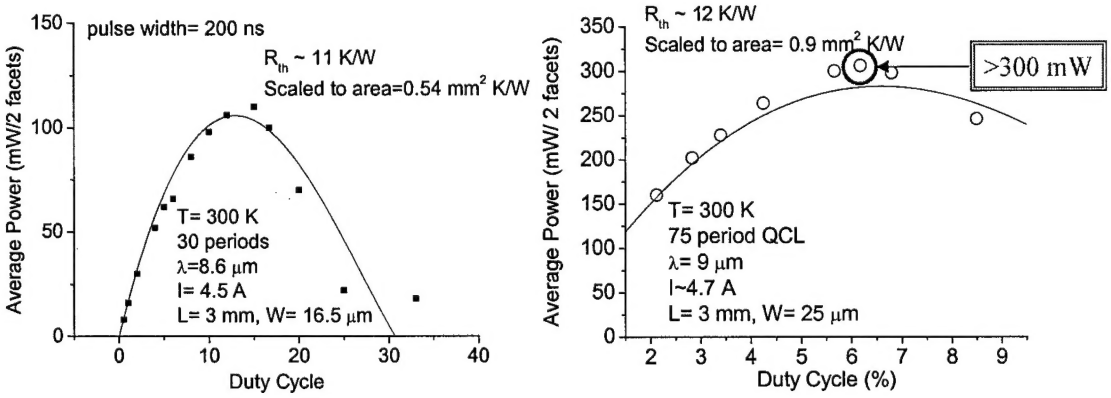

Figure 7 Average power as a function of duty cycle for a) 30 period and b) 75 period QCLs.

Strain-balanced laser results

Another more recent improvement is the addition of strain-balanced QCL lasers. All of the early QCL work was performed using lattice-matched $Ga_{0.47}In_{0.53}As$ / $Al_{0.48}In_{0.52}As$ heterostructures on InP substrate. For shorter wavelength emission (λ <4.5 μm), the conduction band offset of this design (510 meV) is no longer adequate for efficient electron confinement. Rather than move to an entirely new material system, it is possible to increase the conduction band offset locally by selectively lowering/raising the conduction band edge by changing the ternary composition.

In the past, we have shown lasers operating at λ~5 μm with this technique. Preliminary device testing shows very promising results for λ = 6.1 μm lasers as well. Room temperature pulsed operation characteristics are shown in Figure 8. At room temperature we have demonstrated the lowest threshold current density (2.4 kA/cm^2) and highest slope efficiency (586 mW/A), and highest power (2 W peak, 250 mW average) at this wavelength.

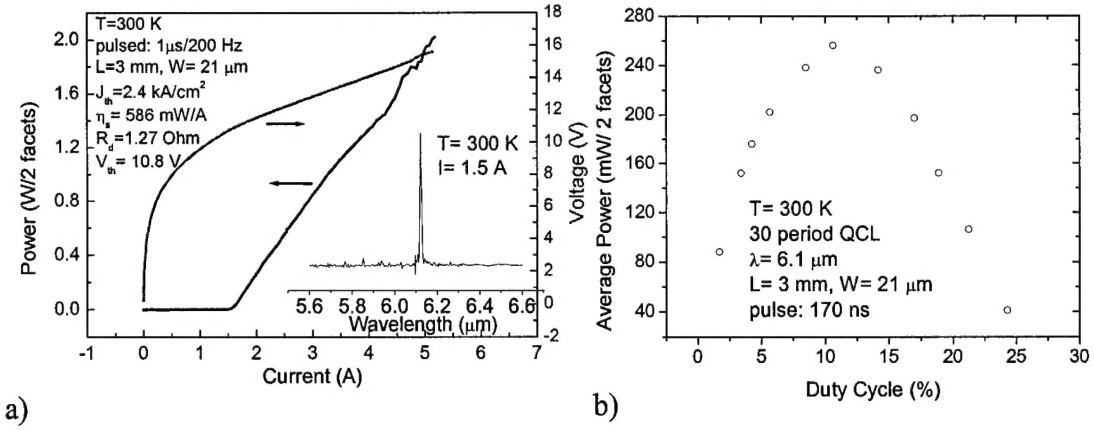

Figure 8 a) Room temperature optical and electrical characteristics of an uncooled 30-period QCL at λ=6.1 μm. b) Average power as a function of duty cycle for the same laser.

Distributed feedback lasers (DFB lasers)

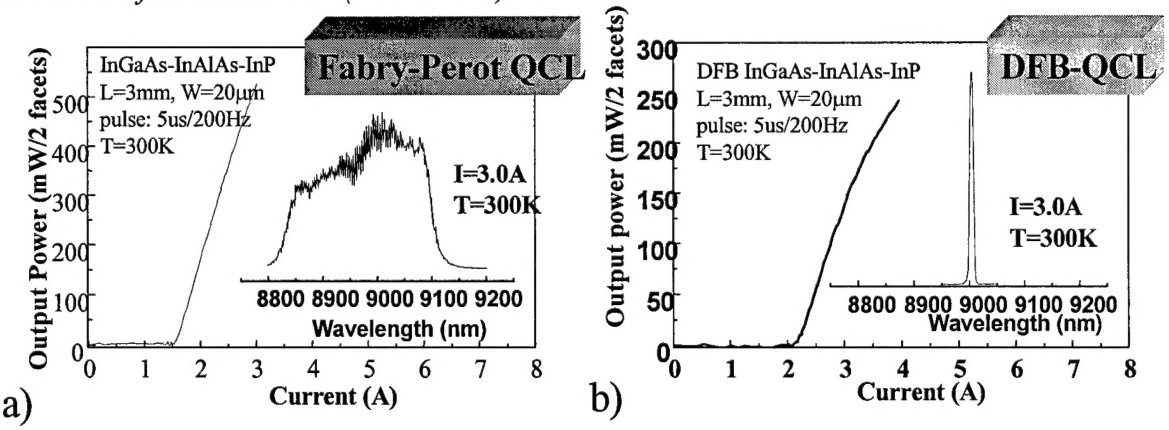

Figure 9 a) Output power vs. current characteristic of λ=9 μm Fabry-Perot QCL at 300 K. Inset shows lasing spectra at 3.0 A. b) Output power vs. current characteristic of λ=9 μm DFB-QCL at 300 K. Inset shows **single mode** lasing spectra at 3.0 A.

Most of the work we have done up to now involves multimode Fabry-Perot lasers. Many strategic applications, however, require single wavelength lasers. In order to preserve a narrow linewidth and inhibit multimode operation, a surface Bragg grating will be incorporated into the laser geometry using electron-beam lithography. Electron beam lithography allows accurate control the grating period and duty cycle. Further, we can experiment with various designs that have been successful in the literature, such as sampled grating and α-DFB lasers. These advanced techniques allow not only single wavelength emission, but also make it possible to add a certain degree of tunability and/or beam divergence control. To date we have successfully demonstrated surface distributed feedback gratings which give single wavelength emission at λ~ 9 μm as shown in Figure 9. At present, the narrowest linewidth achieved in pulsed mode at room temperature is ~3 nm. Further refinement of the

grating technology may show a slightly narrower linewdith, but the narrowset possible linewidth would involve continuous wave operation.

Developing a compact laser pointer system

One of the goals of this project is to produce a compact, room temperature laser pointer system using the quantum cascade laser as a source. In order to accomplish this task, several areas need to be explored, including: design of power system/laser driver, choice of optics, ruggedized mounting and alignment of laser with optics.

The first objective was to design and test an electrical system that can drive a quantum cascade laser. Unfortunately, the QCL power requirements are significantly different than standard near-infrared laser diodes. The QCL requires pulsed operation with amplitudes up to 4 A/ 25V and pulse width <1 μs for efficient operation.

The driving circuit is divided into two section: pulse formation and pulse amplification. The pulse formation stage consists of a 555 timer circuit capable of producing square wave pulses at 200 Hz and a high-speed inverter. The inverter converts the negative pulses of the timer circuit into positive pulses used to drive the amplifier section as shown in Figure 10. The pulse amplification section consists of a fast power MOSFET whose drain is in series with the laser diode. When the inverter output goes high, the MOSFET turns on, which shunts the battery through the laser and a series resistance. The current can be controlled by either adjusting the battery voltage or the series resistance. This arrangement is also shown in Figure 7.

The proposed circuit was designed, constructed, and was successfully used to drive and characterize quantum cascade lasers. The initial circuit ran off a DC power supply, but has since been converted to battery power for pointer integration.

The choice of optics also presents some complications. Compact laser pointers are already well-established in the near-infrared. However, they use custom aspheric glass lenses in order to achieve good performance. The only way this is cost-effective is via mass production. The quantum cascade laser is being developed for a variety of wavelengths, most of which are inaccessible to glass optics due to strong absorption.

The most widely available optics in the 2-12 μm wavelength range are made of Ge and ZnSe. Due to the relatively high refractive index of these materials compared to glass, broadband anti-reflection coatings are needed for system integration. Further, because the pointer should be compact, it is desirable to have small diameter lenses of short focal lengths. These materials can be expensive to manufacture and there are a limited selection of vendors. The additional requirements of coatings and lens size make it nearly impossible to find off-the-shelf components. Further, the manufacturing of custom lenses takes time, which means each evolution of the optics systems can have a long turnaround time.

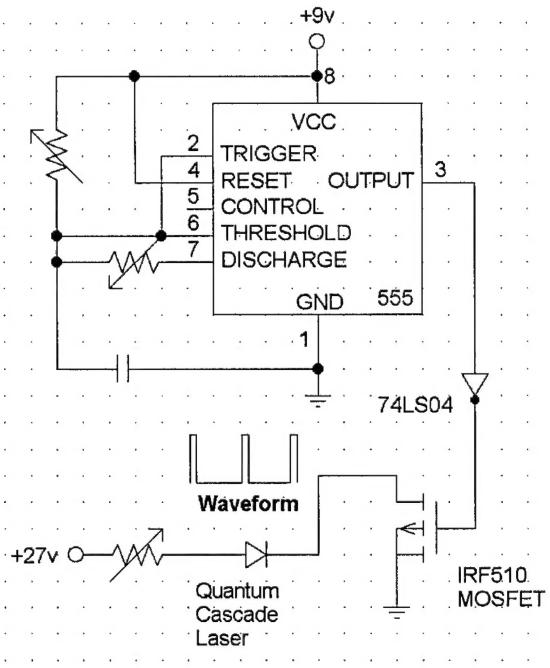

Figure 10 Circuit diagram of quantum cascade laser driver circuit.

A completed pointer is shown in figure along with it's physical specifications. Clearly the batteries (standard 9 V) take up a large volume and there is a significant amount of unused space inside the box. However, this device, which easily fits it the hand, can deliver >1 W of peak power at λ=9 μm.

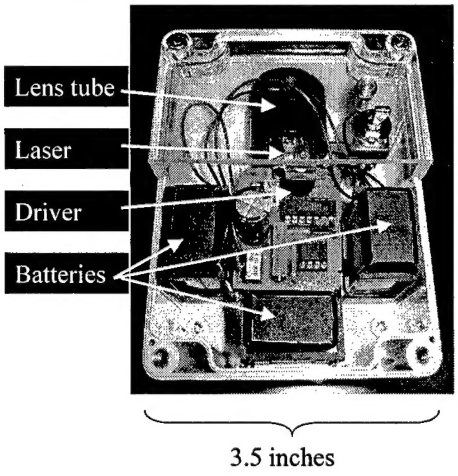

- Pointer Size:
  - 3.5"x4.5"x2.5"
- Weight:
  - 0.910 lbs with batteries
- Input Power Requirements:
  - 9V to power the CMOS driver
  - 27V to power the QCL
  - 0.005 mA average laser current
- Expected Battery Lifetime:
  - 10,000 hours
- Estimated Laser Output Power:
  - >1 W peak (>2 mW average)

Figure 11 Picture of uncooled QCL laser pointer and physical specifications.

The pointer requirements are a collimated beam with <10 mrad divergence. The initial collimation experiment was performed using in-house components. A single 1-inch diameter, f/1 AMTIR lens was used to gauge the difficulty of the objective. A measurement system was also constructed using the materials available in-house, as shown in Figure 12. The laser and lens are mounted on a motorized rotational stage, allowing for adjustment of the lens/laser separation. An irised detector is mounted on an optical rail system facing the laser. The beam divergence in one axis can be

measured by measuring the beam width at two different image planes for a constant lens/laser separation. This measurement was automated in interests of speed. Once the lens is adjusted to give the best collimation, the other axis can be quickly measured by either rotating the laser/lens setup 90 degrees, or by measuring the vertical beam profile using a height-adjustable detector stage. System resolution can be quite good provided the iris opening is small and the detector is distant from the laser.

A superior system would keep the laser and lens fixed and use an infrared focal plane array to measure the beam profile at two image planes. Even continuing with a single element detector, the next generation system would benefit from a motorized detector stage to automate the measurement of both divergence axes.

Using the in-house setup described above, we were able to demonstrate around 5 mrad divergence along the fast axis with 30 μm tolerance in the lens/laser separation. Keeping the optics simple, a vendor was found that could supply a 0.5 inch diameter f/1 ZnSe lens. Assuming the spherical aberrations are low enough to allow similar collimation to the 1-inch lens, we can reduce the pointer size and weight considerably with this new lens.

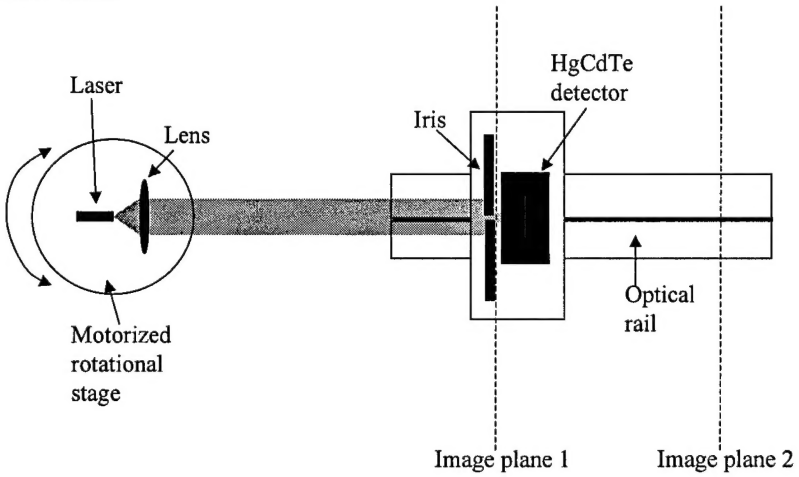

Figure 12 Laboratory setup for measuring divergence of laser/lens combination along one optical axis.

Summary

Under this project we have advanced the state-of-the-art quantum cascade laser performance noticeably. As can be seen form the timeline below (Figure 13), we have made consistent improvement in room temperature threshold current density and peak output power, which are currently among the best reported to date.

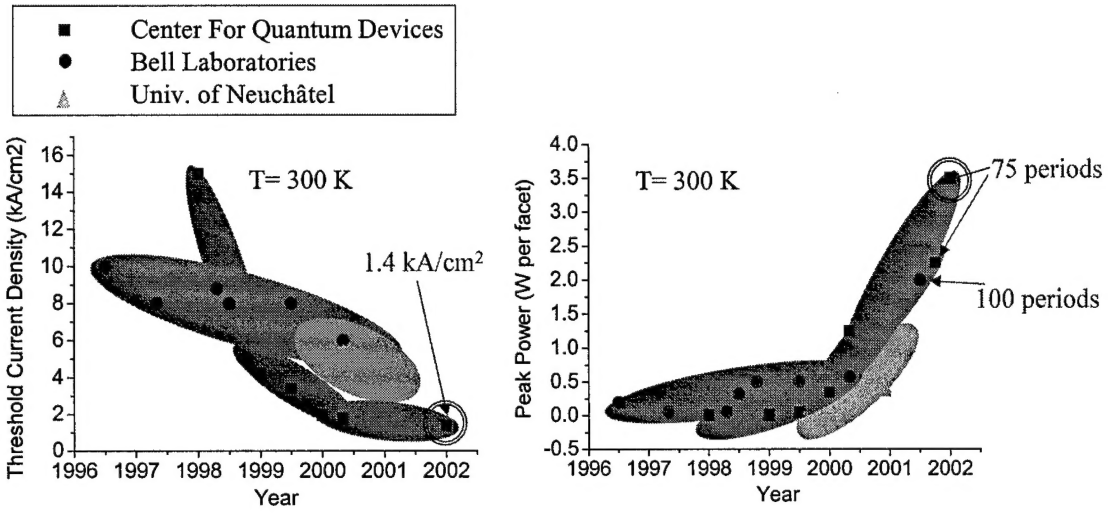

Figure 13 Timeline of progress for $\lambda > 4$ μm quantum cascade laser technology with regards to room temperature threshold current density and peak output power.

We are also advancing the technology by means of a detailed study of grating fabrication using e-beam lithography. Single mode operation has already been demonstrated at both 9 and 11 μm wavelengths. This technology can be expanded into many different forms such as surface emission, infrared WDM, or photonic crystals, which would further increase the QCL's versatility

Finally, we have also completed fabrication of a QCL-based laser pointer, with integrated laser, optics, driver circuitry, and battery power supply. This demonstration is critical to continuing work for QCL integration into chemical spectroscopy, infrared countermeasure, or free-space communication systems.

Future Work

Currently, there is some competition between laser technologies operating in the 3-5 μm spectral range. Lasers are currently being produced with a variety of designs besides the QCL. The most notable of these are based on InAsSbP/InAs/InAsSb superlattices, and Type II GaSb/InAs/AlSb. One of the first tasks to undertake is to develop reliable high-power QCLs in the 3-5 μm spectral range and compare them with these other technologies. The strain-balanced laser results show great promise for lasers in this wavelength range, but further development is required before high power operation can be demonstrated.

Another important step is increasing the average output power of the quantum cascade laser at room temperature. There are both technological and design issues involved, but in the short-term, epilayer down mounting of lasers to copper heatsinks is extremely important. This, and regrowth of thermally conductive material around the active layers, will help to remove heat more effectively and enable higher temperature, higher duty cycle operation.

The laser pointer must also be further developed with these goals in mind. In order to efficiently dissipate the excess heat generated at high duty cycles, a thermal management system must be developed. Further, while pointer applications might require <10 mrad divergence, long-range systems will need to reduce this divergence into